Endothelial thrombomodulin downregulation caused by hypoxia contributes to severe infiltration and coagulopathy in COVID-19 patient lungs

Taejoon Won,[a] Megan K. Wood,[b] David M. Hughes,[c] Monica V. Talor,[a] Zexu Ma,[b] Jowaly Schneider,[a] John T. Skinner,[d] Beejan Asady,[b] Erin Goerlich,[e] Marc K. Halushka,[a] Allison G. Hays,[e] Deok-Ho Kim,[e,f] Chirag R. Parikh,[g] Avi Z. Rosenberg,[a] Isabelle Coppens,[b] Roger A. Johns,[d] Nisha A. Gilotra,[e] Jody E. Hooper,[a] Andrew Pekosz,[b] and Daniela Čiháková[a,b]*

[a]Department of Pathology, Johns Hopkins University School of Medicine, Baltimore, MD 21205, USA
[b]W. Harry Feinstone Department of Molecular Microbiology and Immunology, Johns Hopkins University Bloomberg School of Public Health, Baltimore, MD 21205, USA
[c]Department of Chemical and Biomolecular Engineering, Johns Hopkins University Whiting School of Engineering, Baltimore, MD 21218, USA
[d]Department of Anesthesiology and Critical Care Medicine, Johns Hopkins University School of Medicine, Baltimore, MD 21205, USA
[e]Division of Cardiology, Department of Medicine, Johns Hopkins University School of Medicine, Baltimore, MD 21205, USA
[f]Department of Biomedical Engineering, Johns Hopkins University Whiting School of Engineering, Baltimore, MD 21218, USA
[g]Division of Nephrology, Department of Medicine, Johns Hopkins University School of Medicine, Baltimore, MD 21205, USA

EBioMedicine 2022;75: 103812
Published online xxx
https://doi.org/10.1016/j.ebiom.2022.103812

Summary

Background Thromboembolism is a life-threatening manifestation of coronavirus disease 2019 (COVID-19). We investigated a dysfunctional phenotype of vascular endothelial cells in the lungs during COVID-19.

Methods We obtained the lung specimens from the patients who died of COVID-19. The phenotype of endothelial cells and immune cells was examined by flow cytometry and immunohistochemistry (IHC) analysis. We tested the presence of severe acute respiratory syndrome coronavirus 2 (SARS-CoV-2) in the endothelium using IHC and electron microscopy.

Findings The autopsy lungs of COVID-19 patients exhibited severe coagulation abnormalities, immune cell infiltration, and platelet activation. Pulmonary endothelial cells of COVID-19 patients showed increased expression of procoagulant von Willebrand factor (VWF) and decreased expression of anticoagulants thrombomodulin and endothelial protein C receptor (EPCR). In the autopsy lungs of COVID-19 patients, the number of macrophages, monocytes, and T cells was increased, showing an activated phenotype. Despite increased immune cells, adhesion molecules such as ICAM-1, VCAM-1, E-selectin, and P-selectin were downregulated in pulmonary endothelial cells of COVID-19 patients. Notably, decreased thrombomodulin expression in endothelial cells was associated with increased immune cell infiltration in the COVID-19 patient lungs. There were no SARS-CoV-2 particles detected in the lung endothelium of COVID-19 patients despite their dysfunctional phenotype. Meanwhile, the autopsy lungs of COVID-19 patients showed SARS-CoV-2 virions in damaged alveolar epithelium and evidence of hypoxic injury.

Interpretation Pulmonary endothelial cells become dysfunctional during COVID-19, showing a loss of thrombomodulin expression related to severe thrombosis and infiltration, and endothelial cell dysfunction might be caused by a pathologic condition in COVID-19 patient lungs rather than a direct infection with SARS-CoV-2.

Funding This work was supported by the Johns Hopkins University, the American Heart Association, and the National Institutes of Health.

Keywords: COVID-19; SARS-CoV-2; immunothrombosis; endothelial cell dysfunction; thrombomodulin

*Corresponding author at: Department of Pathology, Johns Hopkins University School of Medicine, 720 Rutland Ave, Ross 648, Baltimore, MD 21205; ORCID ID 0000-0002-8713-2860.
E-mail address: cihakova@jhmi.edu (D. Čiháková).

Introduction

The global pandemic of coronavirus disease 2019 (COVID-19) is caused by a novel severe acute respiratory syndrome coronavirus 2 (SARS-CoV-2) infection that

Research in context

Evidence before this study

Normally functioning endothelial cells protect the blood vessel by preventing unwanted coagulation. In COVID-19 patients, plasma levels of soluble markers associated with endothelial cell activation and dysfunction are elevated. To understand the phenotypic changes of vascular endothelial cells during COVID-19, we searched the PubMed database with the terms "COVID-19 endothelial cells" in combination with "phenotype", "flow cytometry", or "immunohistochemistry". However, there was no article showing a comprehensive profile of endothelial cell phenotype in COVID-19.

Added value of this study

In this study, we report a phenotypic profile of endothelial cells in the COVID-19 patient lungs by using flow cytometry and immunohistochemistry (IHC) analysis. Pulmonary endothelial cells of COVID-19 patients exhibited a dysfunctional phenotype related to thrombosis. Especially, we found a loss of thrombomodulin expression, a potent anticoagulant and anti-inflammatory molecule, in endothelial cells of COVID-19 patients. As a mechanism of endothelial dysfunction in COVID-19, we tested if SARS-CoV-2 can directly infect endothelial cells. We found no clear evidence of SARS-CoV-2 infection in endothelial cells using IHC stain, electron microscopy, and *in vitro* viral infection.

Implications of all the available evidence

These findings provide evidence that endothelial cells may be a critical player to contribute to severe thrombosis in the lungs of COVID-19 patients and that endothelial thrombomodulin expression would be a potential therapeutic target for COVID-19-related immunothrombosis.

primarily affects the respiratory tract.[1] These respiratory effects can range from mild upper respiratory disease to severe pneumonia and acute respiratory distress syndrome (ARDS).[1] However, patients hospitalized with COVID-19 also experienced an increased incidence of venous and arterial thromboembolic complications including acute pulmonary embolism (PE), deep vein thrombosis (DVT), ischemic stroke, or myocardial infarction.[2–4] The incidence of thrombotic complications in intensive care unit patients has been reported between 16 and 49 percent.[2–4] In a meta-analysis of 277 autopsy cases, small vessel thrombi were found in 10·8 percent of cases, and 19·1 percent had macrovascular thrombi such as DVT, PE, and mural thrombi.[5] Patients hospitalized with COVID-19 have elevated levels of D-dimer, a thrombosis biomarker, and fibrin degradation products.[6] Given the prominence of microthrombi in COVID-19, it was proposed to rename COVID-19 as MicroCLOTS (microvascular COVID-19 lung vessels obstructive thromboinflammatory syndrome).[7]

Normally functioning vascular endothelium protects blood vessels by regulating vascular tone and preventing unwanted coagulation, playing an essential role in preventing ARDS.[8,9] Endothelial cells express key molecules that regulate the balance between hemostasis and thrombosis such as thrombomodulin and von Willebrand factor (VWF).[9–12] In COVID-19 patients, elevated plasma levels of soluble VWF, thrombomodulin, intercellular adhesion molecule 1 (ICAM-1), vascular adhesion molecule 1 (VCAM-1), and P-selectin have been shown, suggesting endothelial cell activation and dysfunction.[13–16] Several researchers predicted that vascular endothelial cells in COVID-19 increased adhesion molecule expression for platelet and leukocyte migration and pro-inflammatory cytokine and chemokine production.[8,17,18] Moreover, endothelial cell activation and damage were proposed to play a central role in the pathogenesis of COVID-19 associated with ARDS, vascular leakage, pulmonary edema, and a procoagulant state.[8,18,19] Endothelial cell dysfunction was also expected to cause children's multisystem inflammatory syndrome, which develops in a small percentage of children infected with SARS-CoV-2.[20]

However, the phenotypic and transcriptional changes of endothelial cells in COVID-19 have not been fully described. Many single-cell RNA sequencing (scRNA-seq) studies on COVID-19 were performed with non-tissue samples such as peripheral blood mononuclear cells, bronchoalveolar lavage fluid, nasopharyngeal swab, and sputum, barely containing endothelial cells.[21–25] Several studies using the lung tissues from human or non-human primates have been conducted, but they intended to investigate a host entry for SARS-CoV-2 — angiotensin-converting enzyme 2 (ACE2) and transmembrane serine protease 2 (TMPRSS2) — not showing a comprehensive profile of endothelial cell phenotype and transcriptome.[26–30] Furthermore, endothelial transmembrane molecules such as thrombomodulin and ICAM-1 are generally cleaved by enzymes and released into the blood in diseased conditions, suggesting that a transcriptional profile of endothelial cells would not reflect their dysfunctional phenotype during COVID-19.[11,12,31] Also, it remains unclear whether endothelial cell dysfunction and damage in COVID-19 are induced by direct SARS-CoV-2 infection or indirectly through pathologic conditions such as hypoxia and pro-inflammatory cytokine milieu. Some studies have shown ACE2 expression on endothelial cells with limited evidence for the direct infection by SARS-CoV-2.[32,33] However, others have disputed ACE2 expression on endothelial cells and further infection by SARS-CoV-2.[34–41]

Here, we provide a unique perspective on the phenotypic changes of endothelial cells in the autopsy lungs, hearts, and kidneys of COVID-19 patients using flow cytometry and immunohistochemistry (IHC) analyses.

Pulmonary endothelial cells showed a prothrombotic and dysfunctional phenotype during COVID-19, especially a loss of thrombomodulin expression, an anticoagulant and anti-inflammatory molecule. In addition, macrophages, monocytes, and T cells were increased and activated in the lungs of COVID-19 patients. However, we found no evidence of SARS-CoV-2 infection in the pulmonary endothelium, while the alveolar epithelium exhibited severe SARS-CoV-2 infection and damage, causing hypoxia during COVD-19. We confirmed hypoxic stress on endothelial cells and immune cells in the COVID-19 patient lungs.

Methods

Human samples

We obtained seven lung samples, seven heart samples, and eight kidney samples from nine autopsies of patients who died of COVID-19 at the Johns Hopkins University (Table 1 and Supplementary Table S1). We were unable to collect all three tissues from all patients for technical reasons. As a non-COVID-19 control, eight lung specimens, eleven heart specimens, and ten kidney specimens were obtained from autopsies of patients who had no respiratory, cardiovascular, and renal diseases. Samples were fixed for histology study or cryopreserved for flow cytometry and RT-PCR analysis. For cryopreservation, samples were stabilized in HypoThermosol FRS preservation media (Stemcell) and then frozen in CryoStor CS10 cryopreservation media (Stemcell) at -80°C.

Ethics

Written informed consent was obtained from subjects, and the study protocol was approved by the Committee for the Protection of Human Subjects (IRB NA_00036610). This study was conducted in accordance with the guidelines in the Declaration of Helsinki.

COVID-19 patients	
Number of patients	9
% of males	55·6% (5/9)
Age (years)	66·1 ± 14·2
Ventilation (days)	12·0 ± 12·3
ICU admission (days)	9·9 ± 12·2
Hospitalization (days)	10·6 ± 11·9
SaO_2 (%)	76·8 ± 17·5
CRP (mg/ml)	55·1 ± 46·7
D-dimer (µg/ml)	11·2 ± 12·0
Date of tissue collection	4/7/2020 – 5/2/2020
Controls	
Number of patients	12
% of males	41·7% (5/12)
Age (years)	56·4 ± 18·9

***Table 1*: Clinical and demographic characteristics of patients.**

SARS-CoV-2 *in vitro* infection of primary human endothelial cells

Human coronary artery endothelial cells (HCAECs) were purchased from Cell Applications (300-05a). Cells were cultured in Human Meso Endo Growth Medium (Cell Applications). All infections were performed in a biosafety level (BSL) 3 environment. HCAECs were seeded onto 6-well plates at a density of 200,000 cells/-well. At the time of infection, the growth medium was replaced with media containing SARS-CoV-2 (SARS-CoV-2/USA/DC-HP00007/2020, GISAID EPI_-ISL_434688) at a multiplicity of infection (MOI) of 5 infectious units per cell.[42] Cells were then incubated for 1 hour at 37°C. Media containing the virus was aspirated and replenished with fresh media. Samples were then incubated for 24 hours. Cell images were taken using an EVOS XL Core Imaging System (Invitrogen).

Histology study

Lung, heart, and kidney tissues were paraffin-embedded, cut as 4-μm-thick sections, and stained with H&E. Coagulation abnormalities were graded by microscopic assessment of the severity of thrombus formation (graded from 0 to 5) and hemorrhage (from 0 to 5), and the sum of two item scores was shown. Infiltration was separately scored from 0 to 5. Grading was performed by two independent blinded investigators. Images were acquired on a BX43 microscope (Olympus) with a DS-Fi3 camera (Nikon) using NIS-Elements D Software (Nikon).

Immunohistochemistry staining

The tissue slides were deparaffinized, rehydrated, and blocked with Duel Endogenous Enzyme Block (Dako). Tissue sections were probed with the primary antibody against fibrin (59D8; Millipore), CD42b (SP219; Abcam; RRID: AB_2814749), VWF (F8/86; Invitrogen; RRID: AB_11001165), PECAM-1 (JC/70A; Abcam; RRID: AB_307284), or SARS-CoV-2 spike S1 protein (007; Sino Biological; AB_2827979) and then treated with HRP-conjugated secondary goat anti-rabbit or anti-mouse IgG antibody (Leica). The slides were counterstained with 50% hematoxylin in water.

Cell isolation from autopsy tissue samples

All procedures involving SARS-CoV-2-infected tissue samples were performed in a BSL3 environment until the virus is inactivated. Tissues were minced using a single-edge scalpel and then incubated with 5 mL of tissue digestion enzyme solution for 30 minutes at 37°C with intermittent vortexing. The digestion enzyme solution was prepared with 200 U/ml Collagenase

(Worthington) for lungs or 400 U/ml for hearts and kidneys and supplemented with 50 U/ml DNase I (Worthington) and 50 U/ml Hyaluronidase (Sigma) for all organs. Cells were washed and filtered through 40 μm cell strainers (Falcon).

Flow cytometry

Flow cytometry samples from autopsy tissues were prepared in a BSL3 condition. Single cells were first stained with Live/Dead Fixable Aqua (Invitrogen) and 7-AAD (BioLegend). After blocking with TruStain FcX (BioLegend; RRID: AB_2818986) and normal mouse serum (Invitrogen), cells were surface-stained with fluorochrome-conjugated antibodies (Supplementary Table S2). Cells were then fixed, permeabilized with Cyto-Fast Fix/Perm Buffer (BioLegend), and stained with antibodies against intracellular antigens (Supplementary Table S2). Sample acquisition was performed on a BD FACSymphony flow cytometer (BD) running FACSDiva (BD). Results were analysed using FlowJo software (BD).

Real-time RT-PCR

Total RNA from tissues or cultured cells was extracted using RNeasy Plus Mini Kit (Qiagen) or TRIzol (Invitrogen) in a BSL3 environment. Single−stranded cDNA was synthesized with iScript Reverse Transcription Supermix (Bio-Rad). Target genes were amplified using Power SYBR Green PCR Master Mix (Applied Biosystems), and real-time cycle thresholds were detected via MyiQ2 thermal cycler (Bio-Rad). Data were analysed by the $2^{-\Delta\Delta Ct}$ method and were normalized to *GAPDH* or *HPRT* expression and then to biological controls.

SARS-CoV-2 RNA detection

Total RNA extracted from autopsy tissues or cultured cells were reverse transcribed and then amplified with primers specific for SARS-CoV-2 nucleocapsid (N) genes. Primers for SARS-CoV-2 N1, SARS-CoV-2 N2, and internal control RNase P were obtained from the Integrated DNA Technologies. According to the Centers for Disease Control and Prevention (CDC) guideline, a test is considered positive for SARS-CoV-2 if both SARS-CoV-2 N1 and N2 markers show Ct value <40.

Electron microscopy

The lung tissue was excised from patient autopsies and cut into 2−3 mm^3 pieces, and immediately fixed in 2·5% glutaraldehyde (EM grade; Electron Microscopy Sciences) dissolved in 0·1 M Na cacodylate, pH 7·4, for 2 hours at room temperature. Samples were processed as previously described by the Electron Microscopy Laboratory in the Department of Pathology at the Johns Hopkins University School of Medicine before examination with an electron microscope CM120 (Philips) under 80 kV.[43] Images were acquired with Image Capture Engine V602 (Advanced Microscopy Techniques).

Mice

Wild-type male C57BL/6 mice (JAX 000664) were purchased from the Jackson Laboratory. Mice were housed in specific pathogen-free animal facilities at the Johns Hopkins University School of Medicine. Experiments were conducted with 6- to 10-week-old age-matched mice. For hypoxia exposure, mice were housed in Plexiglas hypoxia chambers with 10·0% O_2 that had continuous airflow.[44] The O_2 concentration was monitored and controlled with a ProOx model 350 unit (BioSpherix) by infusion of N_2. CO_2 and ammonia were removed throughout the experiment. Control mice were exposed to normal room air (20·8% O_2). On day 8 of hypoxia exposure, lungs were perfused with PBS and then harvested. All methods and protocols were approved by the Animal Care and Use Committee of the Johns Hopkins University.

Statistics

GraphPad Prism 8 software was used for statistical analysis. Data shown are mean values of two or three independent experiments. Data were analysed using nonparametric Mann-Whitney test or Kruskal-Wallis test followed by post-hoc Dunn's multiple comparison test. Statistically significant comparisons were represented by asterisks in figures: *P < 0·05; **P < 0·005; ***P < 0·0005. Actual P-values were reported in figure legends. Linear regression using Spearman correlation was tested for correlation analysis. Actual r- and P-values were reported in figures.

Role of the funding source

The funding sources had no involvement in study design, data collection, data analyses, interpretation, or writing of this report.

Results

Coagulation abnormality and infiltration are presented in the lungs of COVID-19 patients

Thromboembolism is the most common pathologic finding in the postmortem lungs of patients who died of COVID-19.[45−48] Thrombus formation is also observed in the autopsy hearts and kidneys from COVID-19 patients.[46,48,49] To test whether thrombosis is present in the lungs, hearts, and kidneys from COVID-19 patient autopsies collected at the Johns Hopkins University, we analysed histologic sections of those tissue specimens. Clinical characteristics of our COVID-19 patient cohort are summarized in Table 1 and Supplementary Table S1. We tested seven lung samples, seven heart samples, and eight kidney samples

collected from the autopsy of COVID-19 patients. Many postmortem lungs from COVID-19 patients showed severe coagulation abnormalities such as vascular congestion, thrombus formation, and hemorrhage, which were not observed in non-COVID-19 autopsy controls (Fig. 1a and Supplementary Fig. S1a). Fibrin deposition normally occurs at the site of the damaged blood vessel during coagulation, however, excessive formation or impaired clearance of a fibrin clot contributes to thrombosis development in pathologic conditions and diseases.[50] IHC studies confirmed the development of fibrin- and platelet-rich thrombi in the lungs of COVID-19 patients (Fig. 1b and c and Supplementary Fig. S1b and c). The autopsy hearts and kidneys of COVID-19 patients exhibited congested blood vessels and fibrin-rich thrombi (Fig. 1a and b and Supplementary Fig. S1a and b). However, the severity of coagulation abnormalities in the hearts and kidneys of COVID-19 patients was milder compared to the lungs (Fig. 1d). No platelet-rich thrombi were found in the hearts and kidneys of COVID-19 patient autopsies (data not shown). Elevated plasma D-dimer levels confirmed thrombosis development in our COVID-19 patient cohort tested upon their hospitalization (Fig. 1e). In addition, we found that the number of platelets in the COVID-19 patient lungs was increased compared with controls by using flow cytometry (Fig. 1f and Supplementary Fig. S2). The number of platelets in the COVID-19 patient lungs was correlated with the severity of hypercoagulability (Fig. 1g). In the hearts and kidneys, the platelet counts were comparable between COVID-19 and control groups (Fig. 1f).

Severe infiltration was another histological finding in the lungs of COVID-19 patients (Fig. 1a). The number of $CD45^+$ infiltrating cells was significantly increased in the COVID-19 patient lungs compared with controls (Fig. 1h and Supplementary Fig. S2). The number of $CD45^+$ cells in the COVID-19 patient lungs analysed by flow cytometry was correlated with the infiltration score histologically graded (Fig. 1i). In contrast, $CD45^+$ cell number was reduced in the hearts of COVID-19 patients compared to controls (Fig. 1h). The kidneys of COVID-19 patients presented a comparable number of $CD45^+$ infiltrating cells to the controls (Fig. 1h). These results indicate that severe hypercoagulability and infiltration develop in the lungs of COVID-19 patients.

Platelets and endothelial cells show a prothrombotic phenotype in COVID-19 patient lungs

To investigate if platelets are activated in the lungs of COVID-19 patients, causing a severe hypercoagulable state, we characterized the phenotype of platelets in the autopsy lungs, hearts, and kidneys. In COVID-19 patients, blood platelets showed upregulated P-selectin and other receptors contributing to aggregation and activation of platelets.[51,52] Our flow cytometry analysis revealed that platelet P-selectin level was increased in the hearts but not in the lungs and kidneys from COVID-19 patient autopsies compared to controls (Fig. 2a and b). We also tested the platelet expression of PF4 (CXCL4), which promotes blood coagulation and is a target of autoantibodies causing heparin-induced thrombocytopenia.[53] Platelet PF4 expression showed a significant increase in the lungs of COVID-19 patients compared to controls (Fig. 2c and d). PF4 level in the heart platelets was also increased in the COVID-19 group, although it was not significant (Fig. 2c and d). In the kidneys, no different PF4 level was found between groups (Fig. 2c and d). Platelet expression of other receptors such as CD40L, CD42b (glycoprotein Ibα), and CXCR4 in the COVID-19 autopsy tissues was comparable to controls (data not shown). In addition, we found a massive production of VWF, a procoagulant, in most COVID-19 patient autopsy tissues – lungs, hearts, and kidneys – using IHC staining (Fig. 2e and Supplementary Fig. S3). VWF was detected in the outer layer of the thrombus and CD31-expressing vascular endothelium in the COVID-19 patient tissues, suggesting VWF expression by both activated platelets and endothelial cells. In contrast, control tissues showed a low level of VWF production only in the vascular endothelial lining (Fig. 2e and Supplementary Fig. S3).

Platelets exhibited an activated phenotype in the lungs, hearts, and kidneys of COVID-19 patients (Fig. 2a-e). However, severe hypercoagulability mainly developed in the lungs of our samples and barely in the hearts and kidneys (Fig. 1a-g). To test whether endothelial cells provide a prothrombotic environment specifically in the lungs during COVID-19, we examined a phenotype of endothelial cells in the lungs, hearts, and kidneys of COVID-19 patients using flow cytometry analysis. We found that endothelial cell expression of anticoagulants thrombomodulin and endothelial cell protein C receptor (EPCR) were significantly downregulated in the lung of COVID-19 patients compared with controls (Fig. 2f-h). Endothelial cells in the hearts of COVID-19 patients showed a slight decrease in thrombomodulin and EPCR expression, but it was not significant (Fig. 2f-h). The kidney endothelial cells expressed thrombomodulin and EPCR with no differences between groups (Fig. 2f-h). In hemostatic conditions, endothelial cells produce nitric oxide and prostaglandin I2 by utilizing the enzymes endothelial nitric oxide synthase (eNOS) and cyclooxygenase 2 (COX-2), respectively, to inhibit platelet aggregation and activation[9]. In the COVID-19 patient organs that we examined, endothelial cells expressed a comparable level of those enzymes to controls (data not shown). Collectively, endothelial cells represent a prothrombotic phenotype in COVID-19 patient lungs, leading to platelet recruitment and coagulation abnormalities.

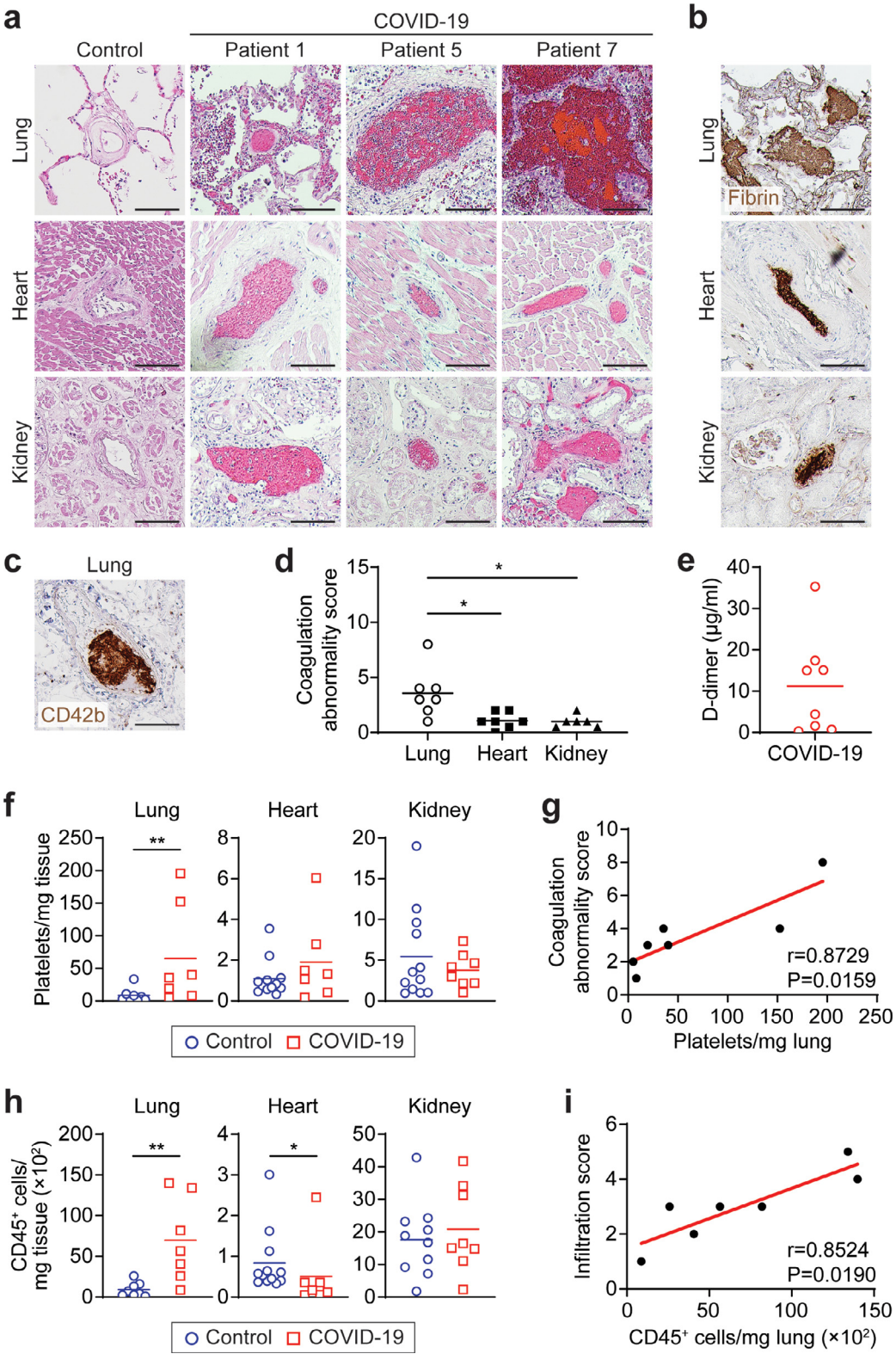

Figure 1. Hypercoagulable state and infiltration in lungs during COVID-19. (a) Representative images of H&E staining on post-mortem lungs, hearts, and kidneys from COVID-19 patients and non-COVID-19 controls. Scale bars: 25 μm. (b) Representative images of immunohistochemistry (IHC) for fibrin (brown) on autopsy lungs, hearts, and kidneys of COVID-19 patients. Scale bars: 25 μm. (c)

Macrophages, monocytes, and T cells are increased and activated in COVID-19 patient lungs

We found an increased $CD45^+$ cell infiltration in the lungs of COVID-19 patients (Fig. 1a and h). To further investigate the immune profile of COVID-19 patient lungs, we analysed the number and phenotype of different immune cells in the autopsy lungs of COVID-19 patients using flow cytometry. Macrophages were the largest immune cell population in both COVID-19 and control lungs and significantly increased in the COVID-19 patients compared with controls (Fig. 3a and Supplementary Fig. S4a). Similarly, the number of monocytes, $CD4^+$ T cells, and $CD8^+$ T cells was increased in the lungs of COVID-19 patients, while the neutrophil count was comparable between COVID-19 and controls (Fig. 3a and Supplementary Fig. S4a). In the phenotype analysis, macrophages in the COVID-19 patient lungs exhibited downregulated HLA-DR expression compared to controls (Fig. 3b and c). CD40 expression on macrophages was increased in the COVID-19 patients, although it was not significant (Fig. 3b and d). Monocytes in the COVID-19 patient lungs revealed upregulated CD16 expression compared with controls but not significantly (Fig. 3e and f). In $CD4^+$ T cells of the COVID-19 patient lungs, $CCR7^+CD45RA^-$ central memory T cells (T_{CM}) were proportionally increased compared to controls, while $CCR7^-CD45RA^+$ effector memory T cells re-expressing CD45RA (T_{EMRA}) were decreased (Fig. 3g and h). However, the absolute number of most $CD4^+$ T cell subsets including $CCR7^+CD45^+$ naÿve T cells (T_N), T_{CM} cells, and $CCR7^-CD45RA^-$ effector memory T cells (T_{EM}) was significantly increased in the COVID-19 patient lungs compared to controls (Fig. 3i). Similarly, the number of $CD4^+$ T_{EMRA} cells was inclined in the COVID-19 patient, although there was no significance (Fig. 3i). The cell frequencies and numbers of $CD8^+$ T cell subsets in the COVID-19 patient lungs exhibited similar results to $CD4^+$ T cells (Supplementary Fig. S4b and c). These data demonstrate that immune cells such as macrophages, monocytes, and T cells are increased and activated in the lungs during COVID-19.

Adhesion molecule expression is reduced in endothelial cells of COVID-19 patient lungs

We and others found increased immune cell infiltration in the autopsy lungs of COVID-19 patients (Fig. 3).[45,48] Several researchers predicted that endothelial cell expression of adhesion molecules such as ICAM-1, VCAM-1, E-selectin, and P-selectin would be upregulated to recruit immune cells in COVID-19.[8,17,18] We tested whether adhesion molecule expression on endothelial cells is altered in the postmortem lungs, hearts, and kidneys from COVID-19 patients. Unexpectedly, endothelial adhesion molecule expression was reduced in the COVID-19 patient lungs compared to controls (Fig. 4a-f). In the lungs, endothelial cells in both COVID-19 and control groups were positive for ICAM-1 (Fig. 4a and b). However, we found a significant downregulation of ICAM-1 in the COVID-19 lungs. Endothelial cells in the control lungs expressed a low level of VCAM-1, E-selectin, and P-selectin, while the COVID-19 lungs showed even lower expression of those molecules (Fig. 4a, c, d, e, and f). In the COVID-19 autopsy hearts, ICAM-1 and E-selectin were significantly downregulated compared to controls, while VCAM-1 and P-selectin expression levels showed no differences (Fig. 4a-f). Endothelial cells in the kidneys from COVID-19 patients expressed a comparable level of adhesion molecules to controls except VCAM-1 (Fig. 4a-f). VCAM-1 was significantly decreased in the COVID-19 kidneys (Fig. 4a and c).

In the COVID-19 patient lungs, a loss of ICAM-1 expression in endothelial cells was not associated with the severity of immune cell infiltration, suggesting that other mechanisms would be involved in the pulmonary infiltration (Fig. 4g). Decreased expression of thrombomodulin in endothelial cells was significantly correlated with an increased infiltration in the lungs of COVID-19 patients (Fig. 4h). Thrombomodulin plays an anti-inflammatory role as well as an anticoagulant function.[11,12,54,55] These data suggest that endothelial cell dysfunction with downregulated adhesion molecules occurs in the lungs of COVID-19 patients and that downregulated thrombomodulin expression in

Representative image of IHC for CD42b (brown) on autopsy lungs of COVID-19 patients. Scale bar: 25 μm. (d) Coagulation abnormality score of COVID-19 patient lungs, hearts, and kidneys examined by H&E stain. Kruskal-Wallis test with Dunn's multiple comparisons test was used for statistical analysis. P-values: 0·0260 (Lung vs Heart); 0·0201 (Lung vs Kidney); 0·9999 (Heart vs Kidney). (e) Plasma D-dimer level in COVID-19 patients upon their hospitalization. (f) Number of platelets in postmortem lungs, hearts, and kidneys from COVID-19 patients and controls determined by flow cytometry. Platelets were gated on $EpCAM^-CD45^-PECAM\text{-}1^{dim}CD41^+$ (Supplementary Fig. S2). Mann-Whitney test was used for statistical analysis. P-values: 0·0205 (Lung); 0·3845 (Heart); 0·9999 (Kidney). (g) Correlation between platelet number and coagulation abnormality score in autopsy lungs of COVID-19 patients. Spearman correlation was used for statistical analysis. (h) Number of $CD45^+$ cells in COVID-19 patient lungs, hearts, and kidneys. $CD45^+$ immune cells were gated on $EpCAM^-CD45^+$ (Supplementary Fig. S2). Mann-Whitney test was used for statistical analysis. P-values: 0·0037 (Lung); 0·0122 (Heart); 0·8286 (Kidney). (i) Correlation between $CD45^+$ infiltrating cell number examined by flow cytometry and infiltration score histologically graded in postmortem lungs of COVID-19 patients. Spearman correlation was used for statistical analysis. In COVID-19 patient group, seven lung samples, seven heart samples, and eight kidney samples were tested. In controls, eight lung samples, eleven heart samples, and ten kidney samples were used. Data shown are mean values of two or three independent experiments. *$P < 0.05$; **$P < 0.005$.

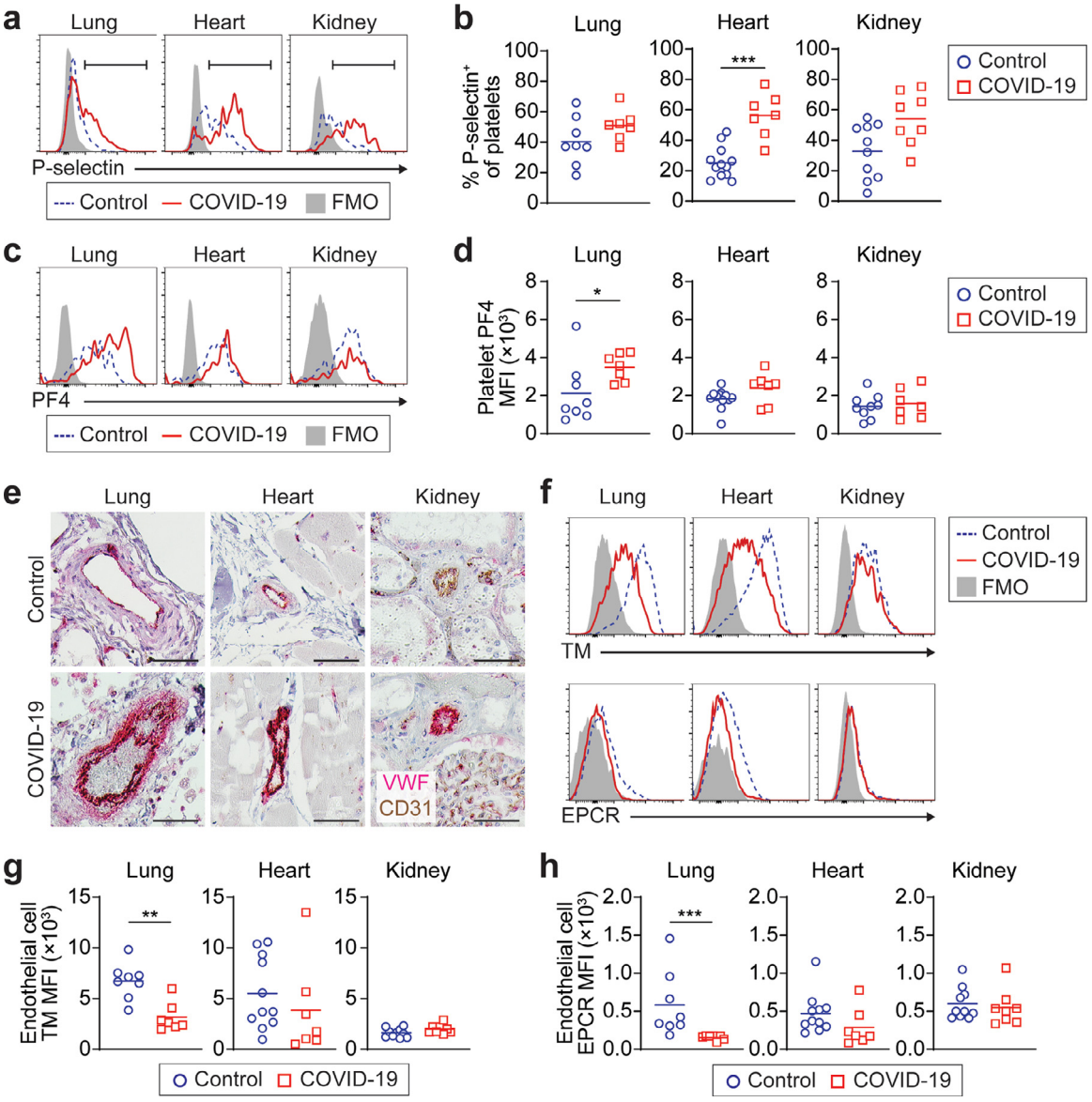

Figure 2. Prothrombotic phenotype of platelets and endothelial cells in COVID-19 patient lungs. (a and b) Flow cytometry analysis (a) and frequencies (b) of P-selectin expression on platelets in lungs, hearts, and kidneys of COVID-19 patients and controls. Platelets were gated on EpCAM$^-$CD45$^-$PECAM-1^{dim}CD41$^+$ (Supplementary Fig. S2). Mann-Whitney test was used for statistical analysis. P-values: 0·2319 (Lung); 0·0003 (Heart); 0·0676 (Kidney). (c and d) Histograms (c) and mean fluorescent intensity (MFI) (d) of PF4 expression in platelets of lungs, hearts, and kidneys from COVID-19 patients and controls. Mann-Whitney test was used for statistical analysis. P-values: 0·0289 (Lung); 0·1422 (Heart); 0·7577 (Kidney). (e) Representative images of immunohistochemistry staining for VWF (red) and CD31 (brown) on lung, heart, and kidney sections from COVID-19 and control autopsies. Scale bars: 12·5 µm. (f) Histograms for thrombomodulin (TM) and endothelial protein C receptor (EPCR) expression on endothelial cells in postmortem lungs, hearts, and kidneys. Endothelial cells were gated on EpCAM$^-$CD45$^-$PECAM-1^{hi}CD34$^+$ (Supplementary Fig. S2). (g and h) MFI of endothelial TM (g) and EPCR (h) expression in lungs, hearts, and kidneys from COVID-19 and control autopsies. Mann-Whitney test was used for statistical analysis. P-values: 0·0022 (Lung); 0·2109 (Heart); 0·1728 (Kidney) (g). P-values: 0·0003 (Lung); 0·0556 (Heart); 0·5884 (Kidney) (h). In COVID-19 patient group, seven lung samples, seven heart samples, and eight kidney samples were tested. In controls, eight lung samples, eleven heart samples, and ten kidney samples were used. Data shown are mean values of two or three independent experiments. *P < 0·05; **P < 0·005, ***P < 0·0005.

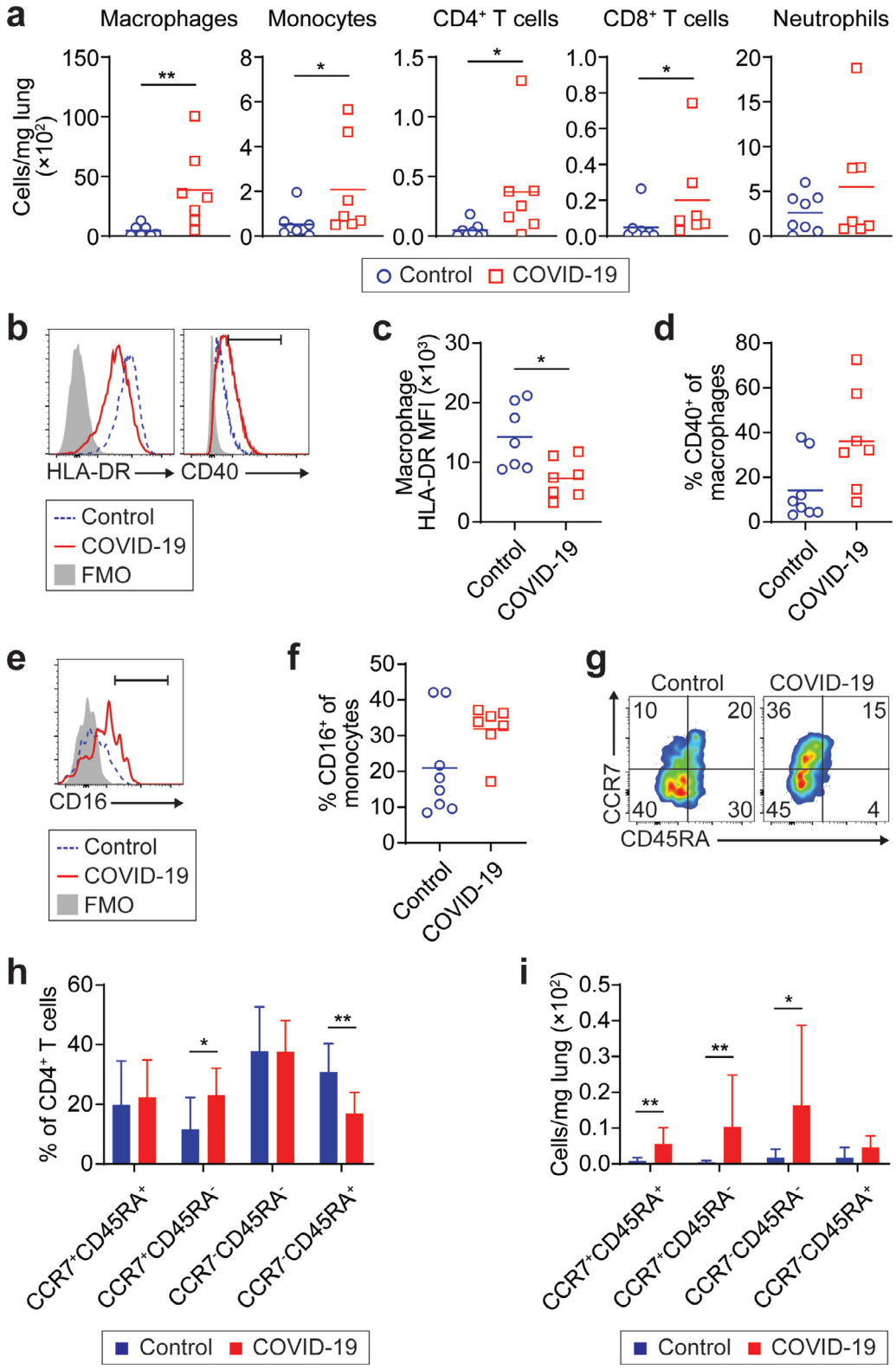

Figure 3. Increased macrophages, monocytes, and T cells with activated phenotype in lungs of COVID-19 patients. (a) Numbers of macrophages ($CD68^+CD206^+$), monocytes ($CD68^+CD206^-CD169^-$), $CD4^+$ T cells ($CD3^+CD4^+$), $CD8^+$ T cells ($CD3^+CD8^+$), and neutrophils ($CD15^+CD66b^+$) in autopsy lungs of COVID-19 patients and controls. The gating strategy for flow cytometry analysis was

endothelial cells is related to severe infiltration during COVID-19.

SARS-CoV-2 does not directly infect endothelial cells or induce their dysfunction

To understand if SARS-CoV-2 directly infects endothelial cells leading to a prothrombotic and dysfunctional state, we first tested the presence of the SARS-CoV-2 genome in the lungs, hearts, and kidneys from COVID-19 patients. All COVID-19 lung specimens were positive for viral RNA in the RT-PCR test (Fig. 5a and Supplementary Fig. S5a). However, two of seven heart samples and six of eight kidney samples tested positive for SARS-CoV-2 RNA (Fig. 5a and Supplementary Fig. S5b and c). Second, we searched SARS-CoV-2 spike protein in the COVID-19 autopsy tissues using IHC stain to detect virus-infected cells. The spike protein was present in all SARS-CoV-2 RNA-positive tissue specimens and was located outside the vascular endothelial layer in the lungs, hearts, and kidneys of COVID-19 patients (Fig. 5b and Supplementary Fig. S5d). Significantly less viral antigen was detected in the heart and kidney tissues compared to the lungs. We could not detect SARS-CoV-2 virions in the vascular endothelium of COVID-19 patient lungs using electron microscopy but were able to identify virus-like particles in the epithelium (Fig. 5c). Those particles represented a SARS-CoV-2-specific ultrastructure described by Miller and Goldsmith.[56] In addition, alveolar epithelial cells of the COVID-19 patients showed an abnormal ultrastructure, which has been observed in ciliary dyskinesia induced by respiratory syncytial virus (RSV) infection (Fig. 5c).[57]

Since endothelial cells of the COVID-19 patient lungs exhibited a prothrombotic and dysfunctional phenotype despite no signs of a direct SARS-CoV-2 infection, we hypothesized that endothelial cell dysfunction is not caused directly by the viral infection. To test this hypothesis, we infected HCAECs with SARS-CoV-2 *in vitro*. HCAECs showed no cytopathic changes at 16 hours post-infection (Fig. 5d). In the RT-PCR test, we found no detectable level of virus RNA in both SARS-CoV-2 and mock infection groups (Supplementary Fig. S5e). Importantly, no downregulation of thrombomodulin, ICAM-1, and VCAM-1 was shown in the SARS-CoV-2-infected HCAECs compared with mock infection control (Fig. 5e). Thus, we did not find evidence of direct endothelial cell infection by SARS-CoV-2 despite a dysfunctional phenotype of endothelial cells in COVID-19 patient lungs.

Epithelial cells are involved in endothelial dysfunction, coagulation, and infiltration in COVID-19 patient lungs

Nasal epithelial cells and type II alveolar epithelial cells in the respiratory system are a primary target of SARS-CoV-2 entry, and the resultant lung injury can cause hypoxia in COVID-19.[58–60] Since we found the SARS-CoV-2 infection and ultrastructural damage in alveolar epithelial cells of COVID-19 patients (Fig. 5c), we tested whether a hypoxic injury occurred in the lungs. In our COVID-19 patient cohort, the average oxygen saturation before death was 76·8% and ranged between 49% and 100% (Fig. 6a, Table 1 and Supplementary Table S1). The mRNA level of *HIF1A*, a hypoxia-induced gene, was upregulated in the COVID-19 patient lungs compared to controls, while the hearts and kidneys showed no differences (Fig. 6b). In the COVID-19 patients, lung epithelial cells showed increased GLUT1 expression, another hypoxia-induced molecule, compared to controls, although epithelial HIF1α expression was comparable between COVID-19 and control groups (Fig. 6c). Endothelial cells and immune cells in the lungs of COVID-19 patients exhibited increased HIF1α and GLUT1 expression, confirming hypoxic stress in the lungs (Fig. 6d and Supplementary Fig. S6). To investigate if hypoxia can directly cause endothelial cell dysfunction in the lungs, we housed naÿve mice in the hypoxia chamber with 10% O_2 for eight days (Fig. 6e). In the hypoxia-exposed mice, the lung endothelial cells showed decreased thrombomodulin and ICAM-1 expression compared to the normal oxygen control, mimicking the dysfunctional phenotype of lung endothelial cells in the COVID-19 patients (Fig. 6f and Supplementary Fig. S7). Other adhesion molecules including VCAM-1, E-selectin, and P-selectin were expressed at comparable levels between the hypoxia and control groups (Fig. 6f and data not shown).

Next, we tested if damaged epithelial cells are directly involved in a hypercoagulable state and

shown in Supplementary Fig. S4a. Mann-Whitney test was used for statistical analysis. P-values: 0·0041 (Macrophages); 0·0140 (Monocytes); 0·0205 ($CD4^+$ T cells); 0·0093 ($CD8^+$ T cells); 0·4634 (Neutrophils). (b) Histograms of macrophage HLA-DR and CD40 expression in COVID-19 patient lungs. (c and d) Mean fluorescent intensity (MFI) of HLA-DR expression (c) and frequency of CD40 expression (d) in lung macrophages from COVID-19 and control autopsies. Mann-Whitney test was used for statistical analysis. P-values: 0·0175 (c); 0·0541 (d). (e and f) Flow cytometry analysis (e) and frequency (f) of CD16 expression in monocytes of autopsy lungs from COVID-19 patients. Mann-Whitney test was used for statistical analysis. P-value: 0·1807. (g) CCR7 and CD45RA expression profiles of $CD4^+$ T cells from COVID-19 and control lungs. (h and i) Frequencies of T cell subsets among $CD4^+$ T cells (h) and absolute numbers (i) in postmortem lungs of COVID-19 patients and controls. Mann-Whitney test was used for statistical analysis. P-values: 0·6943 ($CCR7^+CD45RA^+$); 0·0289 ($CCR7^+CD45RA^-$); 0·6126 ($CCR7^-CD45RA^-$); 0·0037 ($CCR7^-CD45RA^+$) (h). P-values: 0·0037 ($CCR7^+CD45RA^+$); 0·0022 ($CCR7^+CD45RA^-$); 0·0205 ($CCR7^-CD45RA^-$); 0·0721 ($CCR7^-CD45RA^+$) (i). Seven COVID-19 lung samples and eight control lung samples were tested. Data shown are mean values of two or three independent experiments. *P $<$ 0·05; **P $<$ 0·005.

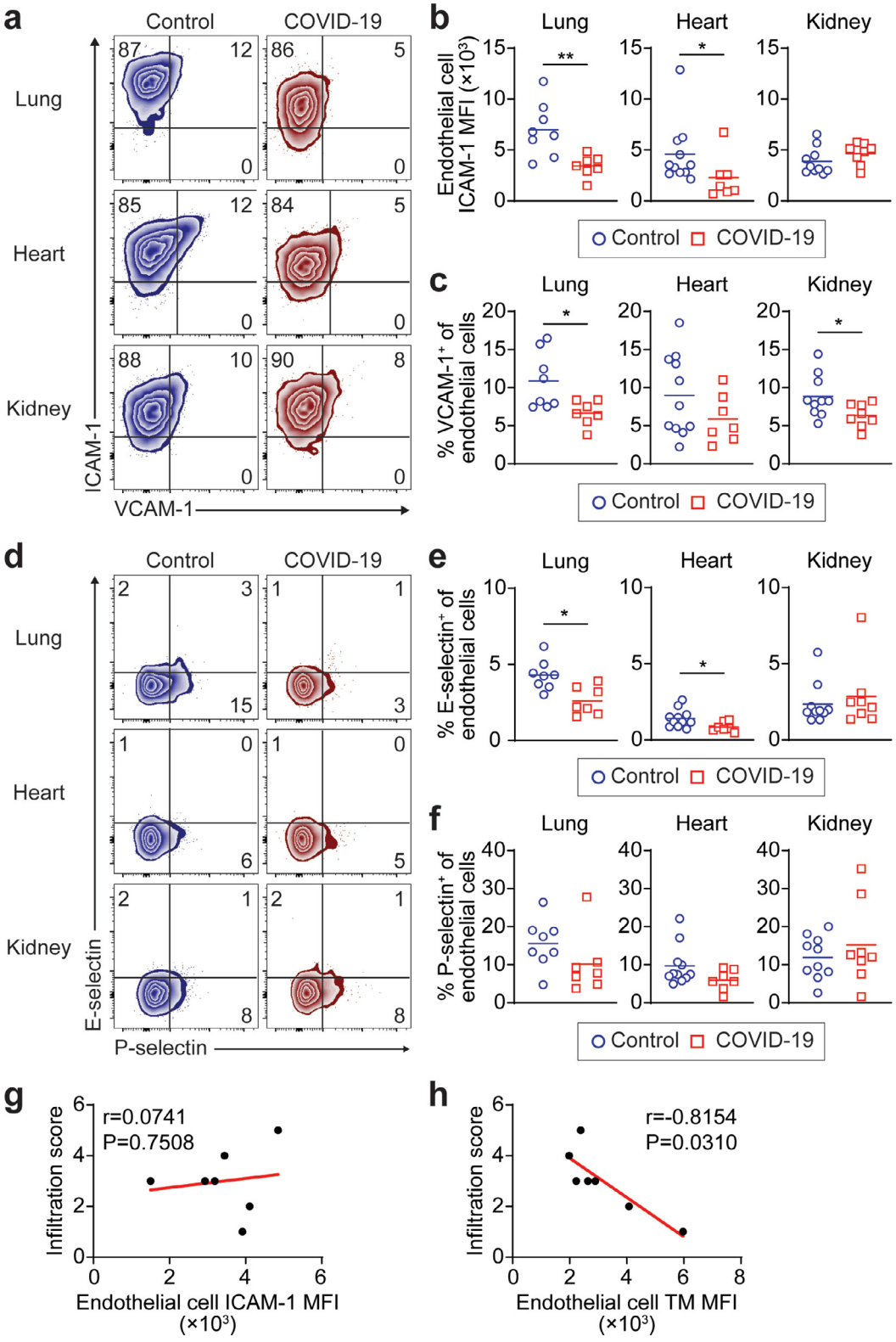

Figure 4. Downregulated adhesion molecules in lung endothelial cells during COVID-19. (a) Flow cytometry analysis of ICAM-1 and VCAM-1 expression on endothelial cells of postmortem lungs, hearts, and kidneys from COVID-19 patients and controls. (b) Mean fluorescent intensity (MFI) of ICAM-1 expression on endothelial cells in lungs, hearts, and kidneys from COVID-19 and control

immune cell infiltration during COVID-19. We found that pulmonary epithelial cells in the COVID-19 patients expressed a higher level of tissue factor, a procoagulant, compared with controls (Fig. 6g and h). Elevated tissue factor expression level in epithelial cells was significantly associated with increased platelet number in the COVID-19 patient lungs (Fig. 6i). In addition, unlike endothelial cells, pulmonary epithelial cells exhibited an increase of ICAM-1 expression in the COVID-19 patients compared to controls, although it was not significant (Fig. 6g and h). These data suggest that pulmonary epithelial cells might participate in endothelial cell dysfunction, platelet activation and aggregation, and immune cell infiltration directly or indirectly via hypoxia during COVID-19.

Discussion

Many researchers have speculated about a phenotype of activated endothelial cells in COVID-19.[8,17,18] However, direct evidence was missing. Most human studies on SARS-CoV-2 infection have used the blood or pharyngeal swab specimens that can be conveniently acquired but barely contain endothelial cells.[61] In this study, we elucidated the dysfunctional phenotype of endothelial cells associated with hypercoagulability and severe infiltration in the lungs during fatal COVID-19. As previously shown by other researchers, we found severe coagulation abnormalities and infiltration in the autopsy lungs from COVID-19 patients.[45–48] Pulmonary endothelial cells exhibited prothrombotic and dysfunctional phenotype with upregulated procoagulant and downregulated anticoagulants and adhesion molecules in COVID-19. However, we were unable to find clear evidence of direct endothelial cell infection by SARS-CoV-2 in the postmortem COVID-19 specimens and the primary cell *in vitro* culture. This suggests that endothelial cell dysfunction might not be directly caused by SARS-CoV-2 infection but rather induced by the pathophysiologic conditions during COVID-19. Unlike the lungs, the hearts and kidneys in COVID-19 showed a mild level of hypercoagulable state, infiltration, and endothelial cell dysfunction.

Several researchers predicted activated and dysfunctional phenotype of endothelial cells showing strong expression of procoagulant VWF in COVID-19.[17,18] Indeed, we found that VWF expression was strikingly increased in endothelial cells of the lungs, hearts, and kidneys from COVID-19 patients. The VWF is a multimeric glycoprotein secreted exclusively by endothelial cells and platelets into the circulation and involved in thrombus formation by tethering platelets to endothelial cells.[9,10] In addition, we found the downregulation of anticoagulants thrombomodulin and EPCR in the lung endothelial cells of COVID-19 autopsies. Thrombomodulin is a transmembrane glycoprotein expressed mainly on endothelial cells but also found in immune cells, vascular smooth muscle cells, keratinocytes, and lung alveolar epithelial cells.[9,11,12] Thrombomodulin is a potent anticoagulant that binds to thrombin and then deactivates it to initiate an anticoagulation cascade. Thrombin-thrombomodulin complex activates protein C, which is a crucial mediator to inactivate coagulant Factors V_a and $VIII_a$ and to further reduce thrombin generation in the anticoagulation processes.[11,12,62] EPCR, another coagulant, presents the protein C to the thrombin-thrombomodulin complex to accelerate protein C activation.[11,62] This suggests that endothelial cell dysfunction with increased procoagulant production and decreased anticoagulant expression is associated with severe thrombus formation and hypercoagulability in the lung of COVID-19 patients.

In the hearts and kidneys of COVID-19 patients, platelets showed an activated phenotype with increased P-selectin, PF4, and VWF expression at a similar level as the lungs. Furthermore, endothelial cells largely produced VWF to a similar degree in the lungs, hearts, and kidneys in the COVID-19 patients. However, the hearts and kidneys from COVID-19 patients exhibited only mild coagulation abnormalities, while the lungs developed fatal thrombosis. This suggests that platelet activation and partial dysfunction of endothelial cells are insufficient for developing a severe multi-organ hypercoagulable state during COVID-19. A loss of thrombomodulin and EPCR expression on endothelial cells seems critical for the progression to fatal thrombotic disorders. Previous studies showed that endothelial expression of those anticoagulant molecules is downregulated in thrombosis associated with meningococcal sepsis, purpura fulminans, and cerebral malaria.[63–65] In mice, endothelial cell-specific thrombomodulin deletion resulted in lethal thrombosis development.[66] We

autopsies. Mann-Whitney test was used for statistical analysis. P-values: 0·0037 (Lung); 0·0154 (Heart); 0·2031 (Kidney). (c) Frequencies of VCAM-1^+ cells among endothelial cells in postmortem lungs, hearts, and kidney specimens. Mann-Whitney test was used for statistical analysis. P-values: 0·0401 (Lung); 0·2463 (Heart); 0·0263 (Kidney). (d) Flow cytometry plots of E-selectin and P-selectin expression on endothelial cells of autopsy lungs, hearts, and kidneys from COVID-19 patients and controls. (e and f) MFI of E-selectin (e) and P-selectin (f) expression in endothelial cells from postmortem lungs, hearts, and kidneys. Mann-Whitney test was used for statistical analysis. P-values: 0·0059 (Lung); 0·0268 (Heart); 0·5726 (Kidney) (e). P-values: 0·0939 (Lung); 0·0853 (Heart); 0·8968 (Kidney) (f). (g and h) Correlation between endothelial ICAM-1 (g) or thrombomodulin (TM) (h) expression and infiltration score histologically evaluated. Spearman correlation was used for statistical analysis. In COVID-19 patient group, seven lung samples, seven heart samples, and eight kidney samples were tested. In controls, eight lung samples, eleven heart samples, and ten kidney samples were used. Data shown are mean values of two or three independent experiments. *$P < 0·05$; **$P < 0·005$.

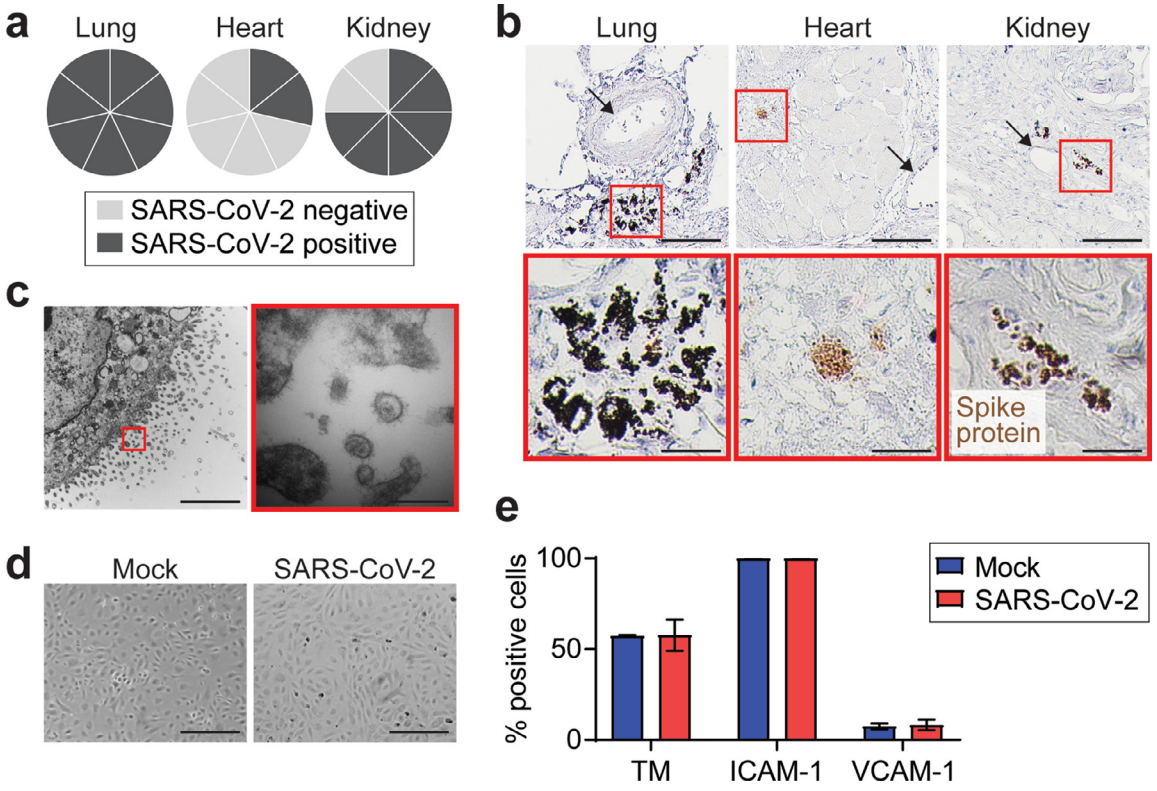

Figure 5. No endothelial cell infection or dysfunction by SARS-CoV-2. (a) Pie charts showing the presence of SARS-CoV-2 RNA tested by RT-PCR in postmortem lungs, hearts, and kidneys from COVID-19 patients. Each pie slice represents one patient. (b) Representative images of immunohistochemistry for SARS-CoV-2 spike protein (brown) on lungs, hearts, and kidneys from COVID-19 autopsies. Scale bars: 25 µm (top); 6·25 µm (bottom). Arrows indicate the blood vessel. (c) Representative images of SARS-CoV-2 in the pulmonary epithelium of COVID-19 patient. Scale bars: 2 µm (left); 200 nm (right). (d) Microscopic images of primary human coronary artery endothelial cells (HCAECs) with *in vitro* SARS-CoV-2 or mock infection. Images were acquired 16 hours after virus inoculation. Scale bars: 125 µm. (e) Frequencies of thrombomodulin $(TM)^+$, ICAM-1^+, and VCAM-1^+ cells among HCAECs with *in vitro* SARS-CoV-2 or mock infection assessed by flow cytometry. Mann-Whitney test was used for statistical analysis. P-values: 0·7000 (TM); 0·9999 (ICAM-1); 0·9999 (VCAM-1). Seven lung samples, seven heart samples, and eight kidney samples were tested. Data shown are mean values of two or three independent experiments.

found a significant loss of thrombomodulin and EPCR expression in the lungs of COVID-19 patients. In contrast, those anticoagulants in the hearts and kidneys were relatively preserved. Recently, decreased endothelial thrombomodulin and ECPR expression in COVID-19 patient lungs was reported by using IHC stain.[67]

In COVID-19 patients, it is reported that the plasma level of soluble thrombomodulin was elevated.[13,15,16] Since pathophysiological conditions such as infection, sepsis, inflammation, and ischemic disease can cause thrombomodulin release from the endothelial cell membrane into the blood, soluble thrombomodulin is considered as a useful biomarker to diagnose endothelial damage and dysfunction.[11,12] Meanwhile, those disease conditions can downregulate endothelial thrombomodulin mRNA transcription through hypoxic stress and pro-inflammatory cytokine milieu.[11] We found hypoxic stress in the endothelial cells of COVID-19 patient lungs. Thus, our finding of decreased thrombomodulin expression on endothelial cells in COVID-19 might be mediated by two regulation processes – release in a soluble form and downregulation of gene transcription.

We elucidated an increase of macrophages, monocytes, $CD4^+$ T cells, and $CD8^+$ T cells in the postmortem lungs of COVID-19 patients using flow cytometry analysis, while other researchers have mainly utilized IHC or scRNA-seq analysis.[68–70] In our analysis, lung macrophages of COVID-19 patients expressed a lower level of HLA-DR and a higher level of CD40 than those of controls. Severe COVID-19 patients showed an increased number of $HLA\text{-}DR^{lo}$ monocytes in the blood, a dysregulated or immunosuppressive subset of monocytes.[25,71-73] This suggests that abnormally or alternatively activated macrophages emerged in the lungs during COVID-19. The role of CD40 expressed on macrophages in COVID-19 remains unclear. However, SARS-CoV-2 infection increased CD40 expression

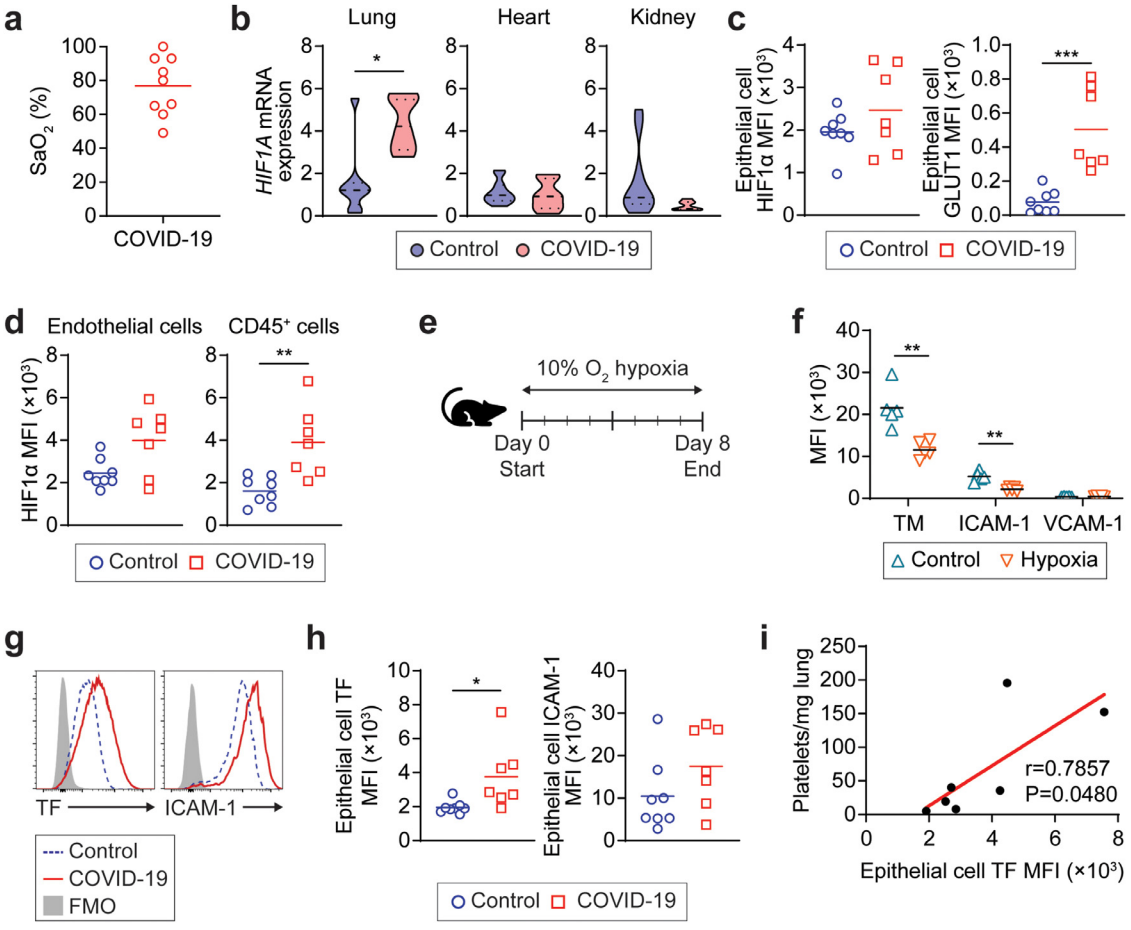

Figure 6. Hypoxic stress induced by activated epithelial cells in lungs of COVID-19 patients. (a) Arterial oxygen saturation (SaO_2) of COVID-19 patients. (b) *HIF1A* gene expression in autopsy lungs, hearts, and kidneys of COVID-19 patients and controls determined by RT-PCR. Mann-Whitney test was used for statistical analysis. P-values: 0·0089 (Lung); 0·5358 (Heart); 0·0553 (Kidney). (c) Mean fluorescent intensity (MFI) of HIF1α and GLUT1 expression on lung epithelial cells in COVID-19 autopsies and controls. Epithelial cells were gated on $EpCAM^+CD45^-$ (Supplementary Fig. S2). Mann-Whitney test was used for statistical analysis. P-values: 0·3969 (left); 0·0003 (right). (d) MFI of HIF1α expression in endothelial cells and $CD45^+$ immune cells in postmortem lungs of COVID-19 patients and controls. Mann-Whitney test was used for statistical analysis. P-values: 0·0541 (left); 0·0012 (right). (e) Scheme of experimental timeline for 10% O_2 hypoxia exposure to C57BL/6 mice. Mice were sacrificed on day 8 of hypoxia. (f) MFI of thrombomodulin (TM), ICAM-1, and VCAM-1 expression on lung endothelial cells collected from mice exposed to hypoxia or normal level of oxygen. Mouse lung endothelial cells were gated on $EpCAM^-CD45^-PECAM\text{-}1^+CD34^+$ (Supplementary Fig. S7). P-values: 0·0079 (TM); 0·0079 (ICAM-1); 0·3095 (VCAM-1). (g) Flow cytometry analysis of tissue factor (TF) and ICAM-1 expression in pulmonary epithelial cells from COVID-19 patients and controls. (h) MFI of TF and ICAM-1 expression in epithelial cells of COVID-19 patient lungs. Mann-Whitney test was used for statistical analysis. P-value: 0·0059 (left); 0·2810 (right). (i) Correlation between epithelial TF expression and platelet number in lungs of COVID-19 patients. Spearman correlation was used for statistical analysis. In COVID-19 patient group, seven lung samples, seven heart samples, and eight kidney samples were tested. In controls, eight lung samples, eleven heart samples, and ten kidney samples were used. In mouse experiment, five mice were used for each group. Data shown are mean values of two or three independent experiments. *P < 0·05; **P < 0·005; ***P < 0·0005.

and decreased HLA-DR expression in M2 macrophages *in vitro*, supporting our findings on the lung macrophages of COVID-19 patients.[74] Our data revealed an increase of $CD16^+$ inflammatory monocytes in the autopsy lungs of COVID-19 patients. Some studies showed an elevated number of $CD14^-CD16^+$ non-classical monocytes in COVID-19 patient blood, while others disagreed.[25,71,75,76] Additionally, we showed that the number of $CD4^+$ T_{EM} and $CD8^+$ T_{EM} cells was significantly increased in the COVID-19 patient lungs. In agreement with this, other studies showed an elevated frequency or number of activated T cells in the blood during COVID-19, although they have used different markers to define T cell subsets than ours.[77,78]

In SARS-CoV-2 infection, it is speculated that vascular endothelial cells exhibit increased expression of adhesion molecules.[8,17,18] ICAM-1 upregulation is generally mediated by various biological stimuli such as inflammation, bacteria or virus infection, and oxidative stress.[79] Endothelial cell expression of other adhesion molecules including VCAM-1, E-selectin, and P-selectin would be increased similarly to ICAM-1 upregulation. In pathologic conditions, adhesion molecules anchored in endothelial cell transmembrane are cleaved by matrix metalloproteinases (MMPs) and released into the blood.[31] Several studies showed that soluble forms of ICAM-1, VCAM-1, E-selectin, and P-selectin are highly elevated in severely ill COVID-19 patients.[13,14] In our flow cytometry analysis, the lung endothelial cells in COVID-19 exhibited reduced expression of surface ICAM-1, VCAM-1, E-selectin, and P-selectin despite increased pulmonary infiltration. It is unclear why adhesion molecule expression was decreased in activated endothelial cells in COVID-19. Since $CD45^+$ cell number was increased in the lungs of COVID-19 patients, it could be hypothesized that endothelial cells upregulate adhesion molecules upon SARS-CoV-2 infection to recruit immune cells from the blood, and then the adhesion molecule expression is downregulated after the infiltration. As a possible cause of downregulation, activated endothelial cells release endothelial microparticles (EMPs), which induce ICAM-1 downregulation on adjacent endothelial cells.[80] In addition, COVID-19 patients showed excessively increased plasma MMP level and enzymatic activity, suggesting the massive cleavage of membrane-bound adhesion molecules on endothelial cells.[81–83] More studies will be necessary to determine how ICAM-1 and other adhesion molecules are downregulated on endothelial cells after the immune cell infiltration in COVID-19. Meanwhile, we found that decreased endothelial thrombomodulin expression was significantly associated with increased infiltration in the lungs of COVID-19 patients, while ICAM-1 expression showed no correlation. Thrombomodulin plays an anti-inflammatory role besides its anticoagulant function by inhibiting immune cell adhesion and suppressing complement system activation.[11,12,54,55] Thus, a loss of thrombomodulin expression on endothelial cells could trigger or accelerate a pathogenic infiltration of immune cells into the lungs during COVID-19.

Since we observed prothrombotic endothelial cells with downregulated adhesion molecule expression in the COVID-19 patient lungs, we wanted to examine the cause of endothelial cell dysfunction. We investigated the hypothesis that SARS-CoV-2 directly infects endothelial cells leading to dysfunction. Although we detected SARS-CoV-2 RNA by RT-PCR test in all autopsy lung specimens with COVID-19, the spike protein was not seen in endothelial cells by IHC stain. We found the SARS-CoV-2 particles in the pulmonary epithelium but not in the endothelium using electron microscopy. Interestingly, the SARS-CoV-2 virions were mostly located around the ciliated epithelium, where highly expresses ACE2 and TMPRSS2 allowing a strong SARS-CoV-2 infection.[22] In addition, we were unable to infect endothelial cells *in vitro* with SARS-CoV-2 or induce endothelial cell dysfunction by the virus infection. Thus, endothelial cells are unlikely to be infected directly by SARS-CoV-2. Several recent studies showed the low susceptibility of endothelial cells to SARS-CoV-2 due to low ACE2 expression.[35–41] This is supported by the fact that recombinant ACE2 transduction is required for sufficient SARS-CoV-2 infection of endothelial cells.[40] Some researchers published electron microscope studies showing SARS-CoV-2 particles present in endothelial cells.[33,47] However, others clarified that those shown particles were indeed cellular ribosomal complexes or vesicles.[34,84]

We sought a pathophysiological condition in SARS-CoV-2 infection that can mediate endothelial cell dysfunction. We found a low oxygen saturation in the COVID-19 patients of our cohort and an increased *HIF1A* gene expression in their lungs, supporting hypoxic stress during COVID-19. The protein levels of HIF1α or GLUT1 were upregulated in epithelial cells, endothelial cells, and immune cells of COVID-19 patient lungs, confirming a hypoxic condition in SARS-CoV-2-infected lungs. Hypoxia can cause endothelial cell dysfunction and further thrombosis.[85,86] In our mouse experiment, hypoxia induced endothelial cell dysfunction exhibiting thrombomodulin and ICAM-1 downregulation, which we observed in the COVID-19 patient lungs. Thus, pulmonary epithelial cells infected and damaged by SARS-CoV-2 could cause hypoxia leading to endothelial dysfunction in COVID-19 patients. Wang *et al.* reported that epithelial cells were more susceptible to SARS-CoV-2 infection compared with endothelial cells in their *in vitro* co-culture system.[38] Co-cultured endothelial cells in the system revealed altered proteomic profile despite no direct SARS-CoV-2 infection, suggesting crosstalk between SARS-CoV-2-infected epithelial cells and endothelial cells. In addition, we found an increased expression of tissue factor and ICAM-1 in pulmonary epithelial cells of COVID-19 patients. Thus, injured epithelial cells may be directly involved in thrombosis and infiltration in the lungs of COVID-19 patients. Alternatively, microparticles derived from platelets, monocytes, and endothelial cells can act as a procoagulant contributing to thrombosis development.[87] Elevated circulating microparticles have been reported in COVID-19 patients, suggesting a pathogenic role of microparticles in COVID-19-related immunothrombosis.[88] Future studies should explore whether microparticles are involved in thrombosis development and further endothelial cell dysfunction in the lungs of COVID-19 patients.

Microbial infection can be a common cause of inflammation-involved thrombosis.[89] Notably, one-half of COVID-19 non-survivors revealed a secondary infection diagnosed by clinical symptoms, signs, or culture tests in Wuhan.[90] In our COVID-19 patient cohort, only two revealed a suspected secondary infection tested by sputum culture, suggesting thrombosis mainly caused by primary SARS-CoV-2 infection or following pathologic conditions.

In this study, we demonstrated the downregulation of endothelial thrombomodulin in the COVID-19 autopsies and suggested a prominent role of thrombomodulin in preventing severe thrombosis and infiltration. In murine models, overexpression of human thrombomodulin or the engineered preservation of thrombomodulin expression protected the lungs from thrombotic disorders and inflammation.[54,91] Moreover, recombinant thrombomodulin or thrombomodulin analog Solulin treatment ameliorated the infarct volume in ischemic stroke.[92,93] Recombinant soluble thrombomodulin administration was also beneficial in patients with disseminated intravascular coagulation and different inflammatory diseases.[12,55,94] Based on our finding of endothelial thrombomodulin downregulation in COVID-19, recombinant thrombomodulin treatment could be considered as a potential therapy.

In conclusion, we found a procoagulant phenotype of endothelial cells with upregulated VWF and downregulated thrombomodulin and EPCR in the lungs and, to a lesser extent, hearts and kidneys during COVID-19. The number of macrophages, monocytes, and T cells was increased in the lungs of COVID-19 patients, and all of them exhibited activated phenotype. Despite increased infiltration, endothelial cell expression of ICAM-1, VCAM-1, E-selectin, and P-selectin was downregulated in the lungs of COVID-19 patients. However, decreased thrombomodulin expression in endothelial cells was related to increased infiltration in the COVID-19 patient lungs. We showed that endothelial cell dysfunction was not caused directly by SARS-CoV-2 infection. Interestingly, we found pulmonary epithelial cell infection and damage by SARS-CoV-2 in the COVID-19 patients. Hypoxia caused by infected epithelial cells would lead to endothelial cell dysfunction in COVID-19. The main limitation of our study is the small sample size. In addition, since we did not have access to biopsy samples of COVID-19 patients, our study was conducted using autopsy specimens. Further studies confirming our findings in fresh biopsy samples from COVID-19 patients are needed.

Contributors

T.W. and D.C. conceptualized study. J.S., C.R.P., A.Z.R., and J.E.H. collected autopsy samples. T.W., M.K.W., D. M.H., M.V.T., Z.M., J.T.S., B.A., I.C., and A.P. performed experiments and analysed data. I.C., A.P., and D.C. verified the underlying data. A.P. supervised BSL3 experiments. T.W. and D.C. wrote the manuscript. E.G., M.K.H., A.G.H., D.-H.K., I.C., R.A.J., N.A.G., J.E. H., A.P., and D.C. reviewed the manuscript and provided intellectual input. All authors reviewed and approved the final version of the manuscript. All authors had full access to all the data in this study and accepted the responsibility to submit for publication.

Declaration of interests

None exist.

Acknowledgments

This work was supported by the Johns Hopkins COVID-19 Research Response Program to D.C. and C.R.P., the COVID-19 Rapid Response Grant 814664 from the American Heart Association (AHA) to D.C., the National Institutes of Health (NIH) Johns Hopkins Center of Excellence in Influenza Research and Surveillance HHSN272201400007C to A.P., the NIH/National Heart, Lung, and Blood Institute (NHLBI) R01HL122606 and NIH/National Institute of General Medicine Sciences (NIGMS) R01GM110674 to R.A.J., and the NIH/National Institute of Diabetes and Digestive and Kidney Diseases (NIDDK) Supplemental Award R01DK093770-09S1 for COVID-19 Research to C.R.P. D.C. is supported by the NIH/NHLBI R01HL118183 and R01HL136586, and AHA 20TPA35490421 and 19TPA34910007. D.C. and N.A. G. are supported by the Matthew Vernon Poyner Memorial Foundation. J.E.H. received support from NIH/National Cancer Institute (NCI) P30CA006973, Cancer Clinical Care support grant and P50CA06924, supplement to a GI SPORE. N.A.G. is supported by the AHA 20SFRN35380046 and NIH/NHLBI R01HL118183. D.-H.K is supported by the NIH/National Institute of Allergy and Infectious Diseases (NIAID) R01AI143773. A.G.H. is supported by NIH/NHLBI R01HL147660. T. W. is supported by the 2018 Rhett Lundy Memorial Research Fellowship from the Myocarditis Foundation. M.K.W. is funded by the NIH/National Institute of Arthritis and Musculoskeletal and Skin Diseases (NIAMS) F31AR077406. D.M.H. is funded by the NIH/NHLBI F31HL149328. The funding sources had no involvement in study design, data collection, analyses, interpretation, or writing of this report.

Data sharing statement

All data reported in this article and supplementary materials are available for sharing by requesting to the corresponding author.

Supplementary materials

Supplementary material associated with this article can be found in the online version at doi:10.1016/j.ebiom.2022.103812.

References

1 Huang C, Wang Y, Li X, et al. Clinical features of patients infected with 2019 novel coronavirus in Wuhan, China. *Lancet* 2020;**395**(10223):497–506.
2 Klok FA, Kruip M, van der Meer NJM, et al. Confirmation of the high cumulative incidence of thrombotic complications in critically ill ICU patients with COVID-19: An updated analysis. *Thromb Res* 2020;**191**:148–50.
3 Middeldorp S, Coppens M, van Haaps TF, et al. Incidence of venous thromboembolism in hospitalized patients with COVID-19. *J Thromb Haemost* 2020;**18**(8):1995–2002.
4 Lodigiani C, Iapichino G, Carenzo L, et al. Venous and arterial thromboembolic complications in COVID-19 patients admitted to an academic hospital in Milan, Italy. *Thromb Res* 2020;**191**:9–14.
5 Halushka MK, Vander Heide RS. Myocarditis is rare in COVID-19 autopsies: cardiovascular findings across 277 postmortem examinations. *Cardiovasc Pathol* 2021;**50**:107300.
6 Tang N, Li D, Wang X, Sun Z. Abnormal coagulation parameters are associated with poor prognosis in patients with novel coronavirus pneumonia. *J Thromb Haemost* 2020;**18**(4):844–7.
7 Ciceri F, Beretta L, Scandroglio AM, et al. Microvascular COVID-19 lung vessels obstructive thromboinflammatory syndrome (Micro-CLOTS): an atypical acute respiratory distress syndrome working hypothesis. *Crit Care Resusc* 2020;**22**(2):95–7.
8 Jin Y, Ji W, Yang H, Chen S, Zhang W, Duan G. Endothelial activation and dysfunction in COVID-19: from basic mechanisms to potential therapeutic approaches. *Signal Transduct Target Ther* 2020;**5**(1):293.
9 Wu KK, Thiagarajan P. Role of endothelium in thrombosis and hemostasis. *Annu Rev Med* 1996;**47**:315–31.
10 Lenting PJ, Christophe OD, Denis CV. von Willebrand factor biosynthesis, secretion, and clearance: connecting the far ends. *Blood* 2015;**125**(13):2019–28.
11 Conway EM. Thrombomodulin and its role in inflammation. *Semin Immunopathol* 2012;**34**(1):107–25.
12 Watanabe-Kusunoki K, Nakazawa D, Ishizu A, Atsumi T. Thrombomodulin as a physiological modulator of intravascular injury. *Front Immunol* 2020;**11**:575890.
13 Goshua G, Pine AB, Meizlish ML, et al. Endotheliopathy in COVID-19-associated coagulopathy: evidence from a single-centre, cross-sectional study. *Lancet Haematol* 2020;**7**(8):e575–e82.
14 Tong M, Jiang Y, Xia D, et al. Elevated expression of serum endothelial cell adhesion molecules in COVID-19 patients. *J Infect Dis* 2020;**222**(6):894–8.
15 Bouck EG, Denorme F, Holle LA, et al. COVID-19 and sepsis are associated with different abnormalities in plasma procoagulant and fibrinolytic activity. *Arterioscler Thromb Vasc Biol* 2021;**41**(1):401–14.
16 Jin X, Duan Y, Bao T, et al. The values of coagulation function in COVID-19 patients. *PLoS One* 2020;**15**(10):e0241329.
17 Lowenstein CJ, Solomon SD. Severe COVID-19 is a microvascular disease. *Circulation* 2020;**142**(17):1609–11.
18 Teuwen LA, Geldhof V, Pasut A, Carmeliet P. COVID-19: the vasculature unleashed. *Nat Rev Immunol* 2020;**20**(7):389–91.
19 Libby P, Luscher T. COVID-19 is, in the end, an endothelial disease. *Eur Heart J* 2020;**41**(32):3038–44.
20 Riollano-Cruz M, Akkoyun E, Briceno-Brito E, et al. Multisystem inflammatory syndrome in children related to COVID-19: A New York City experience. *J Med Virol* 2020.
21 Liao M, Liu Y, Yuan J, et al. Single-cell landscape of bronchoalveolar immune cells in patients with COVID-19. *Nat Med* 2020;**26**(6):842–4.
22 Chua RL, Lukassen S, Trump S, et al. COVID-19 severity correlates with airway epithelium-immune cell interactions identified by single-cell analysis. *Nat Biotechnol* 2020;**38**(8):970–9.
23 Xu G, Qi F, Li H, et al. The differential immune responses to COVID-19 in peripheral and lung revealed by single-cell RNA sequencing. *Cell Discov* 2020;**6**:73.
24 Ren X, Wen W, Fan X, et al. COVID-19 immune features revealed by a large-scale single-cell transcriptome atlas. *Cell* 2021;**184**(7):1895–913. e19.
25 Schulte-Schrepping J, Reusch N, Paclik D, et al. Severe COVID-19 is marked by a dysregulated myeloid cell compartment. *cell* 2020;**182**(6):1419–40. e23.
26 Ziegler CGK, Allon SJ, Nyquist SK, et al. SARS-CoV-2 receptor ACE2 is an interferon-stimulated gene in human airway epithelial cells and is detected in specific cell subsets across tissues. *Cell* 2020;**181**(5):1016–35. e19.
27 Wang A, Chiou J, Poirion OB, et al. Single-cell multiomic profiling of human lungs reveals cell-type-specific and age-dynamic control of SARS-CoV2 host genes. *Elife* 2020;**9**.
28 Singh M, Bansal V, Feschotte C. A single-cell RNA expression map of human coronavirus entry factors. *Cell Rep* 2020;**32**(12):108175.
29 Qi F, Qian S, Zhang S, Zhang Z. Single cell RNA sequencing of 13 human tissues identify cell types and receptors of human coronaviruses. *Biochem Biophys Res Commun* 2020;**526**(1):135–40.
30 Muus C, Luecken MD, Eraslan G, et al. Single-cell meta-analysis of SARS-CoV-2 entry genes across tissues and demographics. *Nat Med* 2021;**27**(3):546–59.
31 Zonneveld R, Martinelli R, Shapiro NI, Kuijpers TW, Plotz FB, Carman CV. Soluble adhesion molecules as markers for sepsis and the potential pathophysiological discrepancy in neonates, children and adults. *Crit Care* 2014;**18**(2):204.
32 Hamming I, Timens W, Bulthuis ML, Lely AT, Navis G, van Goor H. Tissue distribution of ACE2 protein, the functional receptor for SARS coronavirus. A first step in understanding SARS pathogenesis. *J Pathol* 2004;**203**(2):631–7.
33 Varga Z, Flammer AJ, Steiger P, et al. Endothelial cell infection and endotheliitis in COVID-19. *Lancet* 2020;**395**(10234):1417–8.
34 Goldsmith CS, Miller SE, Martines RB, Bullock HA, Zaki SR. Electron microscopy of SARS-CoV-2: a challenging task. *Lancet* 2020;**395**(10238):e99.
35 McCracken IR, Saginc G, He L, et al. Lack of evidence of angiotensin-converting enzyme 2 expression and replicative infection by SARS-CoV-2 in human endothelial cells. *Circulation* 2021;**143**(8):865–8.
36 Chen L, Li X, Chen M, Feng Y, Xiong C. The ACE2 expression in human heart indicates new potential mechanism of heart injury among patients infected with SARS-CoV-2. *Cardiovasc Res* 2020;**116**(6):1097–100.
37 Deinhardt-Emmer S, Bottcher S, Haring C, et al. SARS-CoV-2 causes severe epithelial inflammation and barrier dysfunction. *J Virol* 2021.
38 Wang P, Luo R, Zhang M, et al. A cross-talk between epithelium and endothelium mediates human alveolar-capillary injury during SARS-CoV-2 infection. *Cell Death Dis* 2020;**11**(12):1042.
39 Schaefer IM, Padera RF, Solomon IH, et al. In situ detection of SARS-CoV-2 in lungs and airways of patients with COVID-19. *Mod Pathol* 2020;**33**(11):2104–14.
40 Nascimento Conde J, Schutt WR, Gorbunova EE, Mackow ER. Recombinant ACE2 expression is required for SARS-CoV-2 to infect primary human endothelial cells and induce inflammatory and procoagulative responses. *mBio* 2020;**11**(6).
41 Liu Y, Garron TM, Chang Q, et al. Cell-Type Apoptosis in Lung during SARS-CoV-2 Infection. *Pathogens* 2021;**10**(5).
42 Klein SL, Pekosz A, Park HS, et al. Sex, age, and hospitalization drive antibody responses in a COVID-19 convalescent plasma donor population. *J Clin Invest* 2020;**130**(11):6141–50.
43 Folsch H, Pypaert M, Schu P, Mellman I. Distribution and function of AP-1 clathrin adaptor complexes in polarized epithelial cells. *J Cell Biol* 2001;**152**(3):595–606.
44 Angelini DJ, Su Q, Kolosova IA, et al. Hypoxia-induced mitogenic factor (HIMF/FIZZ1/RELM alpha) recruits bone marrow-derived cells to the murine pulmonary vasculature. *PLoS One* 2010;**5**(6):e11251.
45 Ackermann M, Verleden SE, Kuehnel M, et al. Pulmonary vascular endothelialitis, thrombosis, and angiogenesis in Covid-19. *N Engl J Med* 2020;**383**(2):120–8.
46 Nicolai L, Leunig A, Brambs S, et al. Immunothrombotic dysregulation in COVID-19 pneumonia is associated with respiratory failure and coagulopathy. *Circulation* 2020;**142**(12):1176–89.
47 Bradley BT, Maioli H, Johnston R, et al. Histopathology and ultrastructural findings of fatal COVID-19 infections in Washington State: a case series. *Lancet* 2020;**396**(10247):320–32.
48 Hanley B, Naresh KN, Roufosse C, et al. Histopathological findings and viral tropism in UK patients with severe fatal COVID-19: a post-mortem study. *Lancet Microbe* 2020;**1**(6):e245–e53.

49 Bois MC, Boire NA, Layman AJ, et al. COVID-19-associated Non-Occlusive Fibrin Microthrombi in the Heart. *Circulation* 2020.
50 Kattula S, Byrnes JR, Wolberg AS. Fibrinogen and fibrin in hemostasis and thrombosis. *Arterioscler Thromb Vasc Biol* 2017;**37**(3):e13–21.
51 Bongiovanni D, Klug M, Lazareva O, et al. SARS-CoV-2 infection is associated with a pro-thrombotic platelet phenotype. *Cell Death Dis* 2021;**12**(1):50.
52 Manne BK, Denorme F, Middleton EA, et al. Platelet gene expression and function in patients with COVID-19. *Blood* 2020;**136**(11):1317–29.
53 Arepally GM, Ortel TL. Heparin-induced thrombocytopenia. *Annu Rev Med* 2010;**61**:77–90.
54 Crikis S, Zhang XM, Dezfouli S, et al. Anti-inflammatory and anticoagulant effects of transgenic expression of human thrombomodulin in mice. *Am J Transplant* 2010;**10**(2):242–50.
55 Ito T, Thachil J, Asakura H, Levy JH, Iba T. Thrombomodulin in disseminated intravascular coagulation and other critical conditions-a multi-faceted anticoagulant protein with therapeutic potential. *Crit Care* 2019;**23**(1):280.
56 Miller SE, Goldsmith CS. Caution in identifying coronaviruses by electron microscopy. *J Am Soc Nephrol* 2020;**31**(9):2223–4.
57 Smith CM, Kulkarni H, Radhakrishnan P, et al. Ciliary dyskinesia is an early feature of respiratory syncytial virus infection. *Eur Respir J* 2014;**43**(2):485–96.
58 Sungnak W, Huang N, Becavin C, et al. SARS-CoV-2 entry factors are highly expressed in nasal epithelial cells together with innate immune genes. *Nat Med* 2020;**26**(5):681–7.
59 Mason RJ. Pathogenesis of COVID-19 from a cell biology perspective. *Eur Respir J* 2020;**55**(4).
60 Jahani M, Dokaneheifard S, Mansouri K. Hypoxia: A key feature of COVID-19 launching activation of HIF-1 and cytokine storm. *J Inflamm (Lond)* 2020;**17**(1):33.
61 Dickson RP. Lung microbiota and COVID-19 severity. *Nat Microbiol* 2021;**6**(10):1217–8.
62 Thiyagarajan M, Cheng T, Zlokovic BV. Endothelial cell protein C receptor: role beyond endothelium? *Circ Res* 2007;**100**(2):155–7.
63 Faust SN, Levin M, Harrison OB, et al. Dysfunction of endothelial protein C activation in severe meningococcal sepsis. *N Engl J Med* 2001;**345**(6):408–16.
64 Lerolle N, Carlotti A, Melican K, et al. Assessment of the interplay between blood and skin vascular abnormalities in adult purpura fulminans. *Am J Respir Crit Care Med* 2013;**188**(6):684–92.
65 Moxon CA, Wassmer SC, Milner Jr. DA, et al. Loss of endothelial protein C receptors links coagulation and inflammation to parasite sequestration in cerebral malaria in African children. *Blood* 2013;**122**(5):842–51.
66 Isermann B, Hendrickson SB, Zogg M, et al. Endothelium-specific loss of murine thrombomodulin disrupts the protein C anticoagulant pathway and causes juvenile-onset thrombosis. *J Clin Invest* 2001;**108**(4):537–46.
67 Francischetti IMB, Toomer K, Zhang Y, et al. Upregulation of pulmonary tissue factor, loss of thrombomodulin and immunothrombosis in SARS-CoV-2 infection. *EClinicalMedicine* 2021;**39**:101069.
68 Wang C, Xie J, Zhao L, et al. Alveolar macrophage dysfunction and cytokine storm in the pathogenesis of two severe COVID-19 patients. *EBioMedicine* 2020;**57**:102833.
69 Dorward DA, Russell CD, Um IH, et al. Tissue-specific immunopathology in fatal COVID-19. *Am J Respir Crit Care Med* 2021;**203**(2):192–201.
70 Melms JC, Biermann J, Huang H, et al. A molecular single-cell lung atlas of lethal COVID-19. *Nature* 2021;**595**(7865):114–9.
71 Silvin A, Chapuis N, Dunsmore G, et al. Elevated calprotectin and abnormal myeloid cell subsets discriminate severe from Mild COVID-19. *Cell* 2020;**182**(6):1401–18. e18.
72 Giamarellos-Bourboulis EJ, Netea MG, Rovina N, et al. Complex immune dysregulation in COVID-19 patients with severe respiratory failure. *Cell Host Microbe* 2020;**27**(6):992–1000. e3.
73 Szabo PA, Dogra P, Gray JI, et al. Longitudinal profiling of respiratory and systemic immune responses reveals myeloid cell-driven lung inflammation in severe COVID-19. *Immunity* 2021;**54**(4):797–814. e6.
74 Niles MA, Gogesch P, Kronhart S, et al. Macrophages and dendritic cells are not the major source of Pro-inflammatory Cytokines upon SARS-CoV-2 infection. *Front Immunol* 2021;**12**:647824.
75 Zhang D, Guo R, Lei L, et al. Frontline Science: COVID-19 infection induces readily detectable morphologic and inflammation-related phenotypic changes in peripheral blood monocytes. *J Leukoc Biol* 2021;**109**(1):13–22.
76 Zhou YG, Fu BQ, Zheng XH, et al. Pathogenic T-cells and inflammatory monocytes incite inflammatory storms in severe COVID-19 patients. *Natl Sci Rev* 2020;**7**(6):998–1002.
77 Kuri-Cervantes L, Pampena MB, Meng W, et al. Comprehensive mapping of immune perturbations associated with severe COVID-19. *Sci Immunol* 2020;**5**(49).
78 Thevarajan I, Nguyen THO, Koutsakos M, et al. Breadth of concomitant immune responses prior to patient recovery: a case report of non-severe COVID-19. *Nat Med* 2020;**26**(4):453–5.
79 Rahman A, Fazal F. Hug tightly and say goodbye: role of endothelial ICAM-1 in leukocyte transmigration. *Antioxid Redox Signal* 2009;**11**(4):823–39.
80 Jansen F, Yang X, Baumann K, et al. Endothelial microparticles reduce ICAM-1 expression in a microRNA-222-dependent mechanism. *J Cell Mol Med* 2015;**19**(9):2202–14.
81 Abers MS, Delmonte OM, Ricotta EE, et al. An immune-based biomarker signature is associated with mortality in COVID-19 patients. *JCI Insight* 2021;**6**(1).
82 Ueland T, Holter JC, Holten AR, et al. Distinct and early increase in circulating MMP-9 in COVID-19 patients with respiratory failure. *J Infect* 2020;**81**(3):e41–e3.
83 Syed F, Li W, Relich RF, et al. Excessive matrix metalloproteinase-1 and hyperactivation of endothelial cells occurred in COVID-19 patients and were associated with the severity of COVID-19. *J Infect Dis* 2021;**224**(1):60–9.
84 Dittmayer C, Meinhardt J, Radbruch H, et al. Why misinterpretation of electron micrographs in SARS-CoV-2-infected tissue goes viral. *Lancet* 2020;**396**(10260):e64–e5.
85 Mackman N. New insights into the mechanisms of venous thrombosis. *J Clin Invest* 2012;**122**(7):2331–6.
86 Bovill EG, van der Vliet A. Venous valvular stasis-associated hypoxia and thrombosis: what is the link? *Annu Rev Physiol* 2011;**73**:527–45.
87 Owens 3rd AP, Mackman N. Microparticles in hemostasis and thrombosis. *Circ Res* 2011;**108**(10):1284–97.
88 Morel O, Marchandot B, Jesel L, et al. Microparticles in COVID-19 as a link between lung injury extension and thrombosis. *ERJ Open Res* 2021;**7**(2).
89 Beristain-Covarrubias N, Perez-Toledo M, Thomas MR, Henderson IR, Watson SP, Cunningham AF. Understanding infection-induced thrombosis: lessons learned from animal models. *Front Immunol* 2019;**10**:2569.
90 Connors JM, Levy JH. COVID-19 and its implications for thrombosis and anticoagulation. *Blood* 2020;**135**(23):2033–40.
91 Wu Z, Liu MC, Liang M, Fu J. Sirt1 protects against thrombomodulin down-regulation and lung coagulation after particulate matter exposure. *Blood* 2012;**119**(10):2422–9.
92 Su EJ, Geyer M, Wahl M, et al. The thrombomodulin analog Solulin promotes reperfusion and reduces infarct volume in a thrombotic stroke model. *J Thromb Haemost* 2011;**9**(6):1174–82.
93 Nakamura Y, Nakano T, Irie K, et al. Recombinant human soluble thrombomodulin ameliorates cerebral ischemic injury through a high-mobility group box 1 inhibitory mechanism without hemorrhagic complications in mice. *J Neurol Sci* 2016;**362**:278–82.
94 Yamakawa K, Aihara M, Ogura H, Yuhara H, Hamasaki T, Shimazu T. Recombinant human soluble thrombomodulin in severe sepsis: a systematic review and meta-analysis. *J Thromb Haemost* 2015;**13**(4):508–19.